Impact of Assimilating Radar Radial Wind in the Canadian High Resolution Ensemble Kalman Filter System

12B.5

Kao-Shen Chung [1,2], Weiguang Chang [1], Luc Fillion [1,2], Seung-Jong Baek[1,2]
[1] Department of Atmospheric and Oceanic Sciences, McGill University
[2] Meteorological Research Branch, Environment Canada

1. Introduction

Although weather radars provide a large amount of data at high spatial and temporal resolution, assimilating them effectively is quite challenging. Given reflectivity and radial velocity as the only two types of radar observations, forecast model variables such as temperature and humidity are not directly observed by radars, but still require significant analysis corrections. Therefore, information needs to transfer correctly from observations to unobserved variables. Then ensemble Kalman Filter (EnKF) is appropriate for this task since it applies Monte Carlo theory on ensemble members to infer the statistical relationships between errors of observed and unobserved variables.

A High Resolution Ensemble Kalman Filter (HREnKF) is implemented for assimilating radar observations with the Canadian Meteorological Center (CMC)'s Global Environmental Multiscale Limited Area Model (GEM-LAM). The HREnKF system covers the Montréal region with McGill radar located near the center of the domain. As a first step towards full radar data assimilation, only radial velocities are directly assimilated in this study. The HREnKF is carefully applied under different weather conditions. Its impact on analysis and short-term forecasts is addressed.

2. Description of HREnKF for radar data assimilation

2.1 Assimilation system

The HREnKF inherits from the global EnKF scheme implemented operationally at the Canadian Meteorological Center (Houtekamer et. al 2005), and the fundamental HREnKF algorithm can be described by the following set of equations:

$$\boldsymbol{X}_j^f = \mathcal{M}(\boldsymbol{X}_j^a + \varepsilon_j) \tag{2.1}$$

$$\mathbf{K}_i = var(\mathbf{X}_{j'}^f, \mathbf{H}\mathbf{X}_{j'}^f)(var(\mathbf{H}\mathbf{X}_{j'}^f, \mathbf{H}\mathbf{X}_{j'}^f) + \mathbf{R})^{-1} \tag{2.2}$$

$$\mathbf{X}_j^a = \mathbf{X}_j^f + \mathbf{K}_i(\mathbf{O}_j - \mathbf{H}\mathbf{X}_j^f), \tag{2.3}$$

where i =1, 2, …, is a subgroup index; j and j' represent the indices of ensemble members within and outside the subgroup i respectively. The matrix $\boldsymbol{K}_i$ is the Kalman gain used in subgroup i, and calculated from all the ensemble members other than the ones in i. Superscripts a and f represent analysis and forecast (i.e. background) respectively; **X** is the model state vector; $\boldsymbol{O}_j$ represents perturbed observation vector; **H** stands for the observation operator; R is the observation error covariance matrix; $\mathcal{M}$ is the nonlinear forecast model; ε_j represents random perturbations added onto each analysis member to simulate model errors. The error covariance matrices in Eq. (2.2) are estimated from

$$var(\mathbf{A}_j, \mathbf{B}_j) = \rho \circ \frac{1}{N-1} \sum_{j=1\ldots N} (\mathbf{A}_j - \overline{\mathbf{A}})(\mathbf{B}_j - \overline{\mathbf{B}})^T \tag{2.4}$$

where ρ represents the localization function which will be explained later and $\rho \circ$ means a Schur product with the localization function (Houtekamer and Mitchell 2001).

Besides the basic equations, the HREnKF system's characteristics involve four subgroups of ensemble members, three-dimensional localization, a sequential assimilation process and background check (see details in Chung et. al 2013).

Basically, the HREnKF operates as shown in Fig.1. HREnKF starts from 80 initial ensemble members. After ensemble members are ready, HREnKF drives them to go through one forecast step and one analysis step in every analysis cycle. During the forecast step, random perturbations representing model errors are applied to ensemble members to prevent ensemble spread reduction. Since model errors at the convective scale are not well understood, they are simply simulated here by homogenous and isotropic Gaussian distributed random fields (Chung et al. 2013). Given the 80 perturbed members as initial conditions, the high resolution GEM-LAM is integrated for five minutes to yield 80 ensemble forecasts that are considered as 80 background fields ready for the analysis step. In the analysis step, 80 sets of observations are generated by perturbing real observations. They are then statistically combined with the background using the EnKF equations (Eqs. 2.2 and 2.3) to produce 80-member ensemble analysis, from which an ensemble of

* *Corresponding author address*: Kao-Shen Chung, Atmospheric and Oceanic Sciences, McGill University, 805 Sherbrooke W., Montreal, QC. H3A 2K6, Canada;
E-mail: kao-shen.chung@mail.mcgill.ca

forecasts can be periodically performed. The above processes compose the first cycle, after which the ensemble analysis goes to the next cycle.

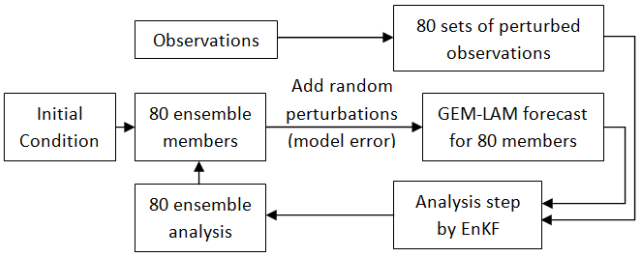

Fig 1. Flow chart of HREnKF.

2.2 GEM-LAM configurations

The fully compressible limited area model GEM-LAM at 1-km resolution is used with integration time step of 30 s in our study. The model employs an implicit scheme in time and a semi-Lagrangian advection scheme. The limited area simulations are fully non-hydrostatic with 58 hybrid vertical levels and a lid at 10 hPa. As opposed to the multi-model option (different versions of physical parameterizations for different ensemble members) used in the global EnKF system, the HREnKF system currently keeps all the physical schemes fixed for model integration. The double-moment version of the Milbrandt and Yau (2005) microphysics scheme is used for the grid-scale processes. The model control variables include horizontal winds, temperature, specific humidity, vertical velocity, mixing ratio and number concentration of six hydrometeor variables (cloud water, rain, snow, ice, graupel and hail).

2.3 Radar observations and observation operator

In this study, the radar observations assimilated by HREnKF are provided from the S-band dual-polarized Doppler radar at J. S. Marshall Radar Observatory operated by McGill University. Before radar data are brought to the HREnKF system, J. S. Marshall Radar Observatory uses polarization information and mathematical algorithms to remove the data contamination including ground clutter, blockage effect, Doppler ambiguity and range folding. The measurement error of radial velocity after the cleaning process is estimated to have a standard deviation of 1 m/s. This value is taken in HREnKF as observation error. After quality control, data thinning is applied to radar data to ensure observation errors are uncorrelated. Firstly, although the original observation errors from McGill radar are correlated, their correlation structures are not fully known. Therefore, it is convenient to assume no correlation among observation errors. Secondly, the sequential assimilation process of HREnKF is only valid under the condition that the observation errors in different batches are independent. Thus, a 4-km data thinning is applied in three dimensions on the radar data. After data thinning, around one third of observations are kept from raw data.

The observation operator basically maps model variables to observation space. Radial velocities, the only type of observation directly assimilated in the current HREnKF, can be written as a function of three wind components as shown in Eq. (2.5).

$$V_r = U\sin(\varphi)\cos(\theta) + V\cos(\varphi)\cos(\theta) + (W + V_t)\sin(\theta) \quad (2.5)$$

where U, V and W are three wind components from model output; V_t is terminal velocity; φ and θ are azimuth and elevation angles respectively. Similar to other studies in the literature (e.g. Sun and Crook 1997, Chung et al. 2009), V_t is calculated from reflectivity observations. Although reflectivity data are not assimilated directly by HREnKF, they are used in the observation operator for the calculation of radial velocity.

3. Design of the experiments

3.1 Experimental design

The experiment procedure consists of 1-hour HREnKF cycling and 1.5-hour short-term ensemble forecasts, which are synchronous with a 2.5-h control run (Fig. 2). The HREnKF cycling process begins with 5-min model integration of the 80 initial ensemble members; then assimilates observations of radial velocity every 5 minutes for 12 cycles; and finally produces an ensemble of analyses. The short-term 80-member ensemble forecasts is initiated from the final analysis ensemble and lasts for 90 minutes. To investigate the impact of radial velocity assimilation by HREnKF on analysis and forecast, a control run is established during the same entire experimental period.

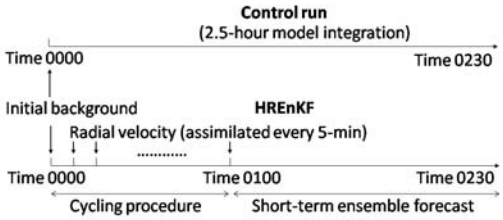

Fig. 2. Experiment procedure. Time 0000 indicates the start of the experiment, not the real time. Time 0230 indicates 2 hours and 30 minutes after the start of the experiments.

It is now better documented in the literature (Saito et al. 2012, Caron 2013) that perturbing lateral boundary conditions in ensemble forecast systems is important. Therefore, since a regional EnKF-15km system (referred to as RENKF) is currently available in research mode at EC, the approach assigns each member of HREnKF different lateral boundary conditions from the members of the REnKF. The latter assimilates conventional observations (same type as the global EnKF) every 6 hours for two cycles, the final ensemble analysis of which is used to generate the initial 80 ensemble members for HREnKF (see flow chart in Fig. 3).

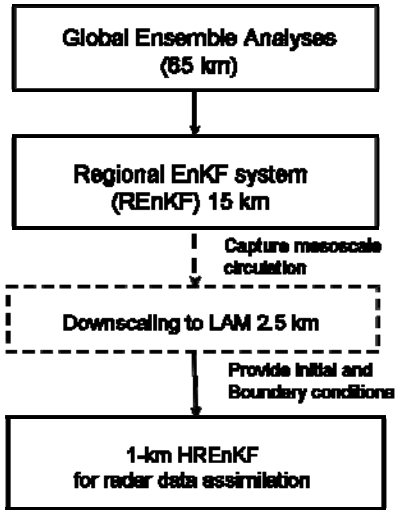

Fig. 3. Flow chart of the HREnKF experiment with the application of the regional EnKF for capturing mesoscale circulation and providing initial and lateral boundary conditions to the HREnKF.

3.2 Description of case study

HREnKF is applied to three different summer cases for the purpose of examining its impact on analysis and forecast under different weather conditions (i.e. squall line structure; isolated small-scale structure; and wide spread stratiform system). In this extended abstract, we present a case happened on June 12 2011 where severe storms stroke the Montréal area in the afternoon, and delayed the "Grand Prix de Formule Un" car racing for more than two hours. As seen in the radar image (Fig. 4), scattered storms near the center of the domain were small-scale, isolated and strong. Those storms moved from southwest to northeast and lasted for many hours. On the southern portion of the domain, a well organized stratiform weather system already existed and gradually decayed. HREnKF is performed from 1600 UTC to 1700 UTC. The short-term forecast is from 1700 UTC to 1830 UTC.

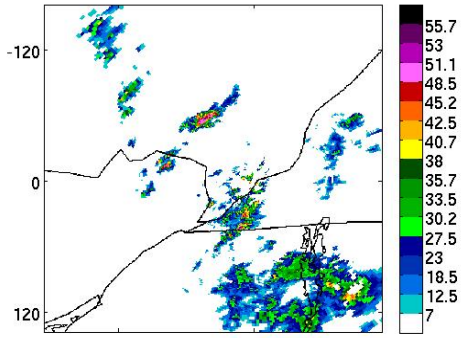

Fig. 4. Reflectivity observations on the 4th elevation angle of June 12, 2011 at 1700 UTC.

4. Results

4.1 Analysis increments

Figure 5 shows the one-step increments (subtracting forecast from analysis at the analysis step, A-P) of V-component of the wind and humidity in the third cycling step at 1615UTC. As directly involved in the observation operator (Eq. 2.5), the V-component is partly observed by the radar, and thus can be directly updated by assimilating radial velocities. On the other hand, the humidity field does not appear in the observation operator equation, and therefore requires cross-correlation between errors of humidity and observed variables (e.g. U, V components) to be updated. The increment of humidity is up to 0.5 g/Kg at some locations in Fig.5b (e.g. to the southwest of the radar), a value big enough to trigger convection under certain conditions (evidence of this in a parameterized convection context is given in Fillion and Bélair 2004).

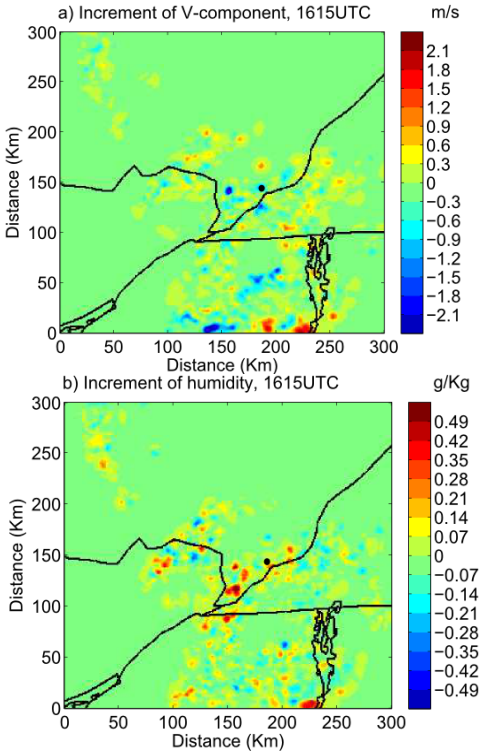

Fig. 5. The increments of V-component and humidity fields close to the surface in the third cycle at 1615 UTC, on June 12, 2011. The black dot denotes the location of radar.

4.2 Ensemble Spread and rms errors

The ensemble spread and rms errors of analysis and background during the cycling process are shown in Fig.6a, where no severe ensemble spread insufficiency appears. In addition, the observation-pass-ratios, which

is defined as the ratio of the number of observations which pass the background check to the total observation number available for each cycling step is plotted in Fig.6b. The result shows that larger portions of observations pass the background check as more cycles are involved, indicating that background fields tend to gradually converge to observations.

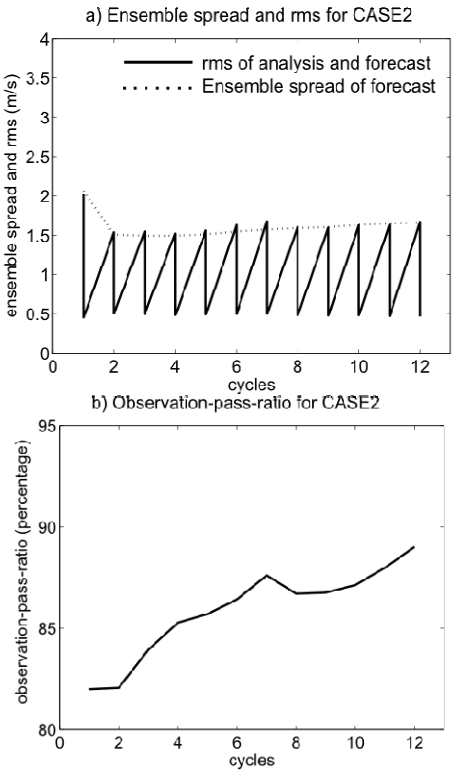

Fig. 6. Results of cycling process the case of June 12, 2011. a) Ensemble spread (dashed line), background rms (12 upper points on the solid line) and analysis rms (12 lower points on the solid line) during the cycling process. b) observation-pass-ratio.

4.3 Verification

The effect of HREnKF on analysis and short-term forecast is demonstrated by scores of radial wind bias and rms in Fig.7. At 1700 UTC, the values of bias and rms for analyses are generally much smaller than those for the control run (Fig.7a), and such patterns last until 18:30 UTC for 90 min (Fig. 7 b, c, d) during short-term forecasts.

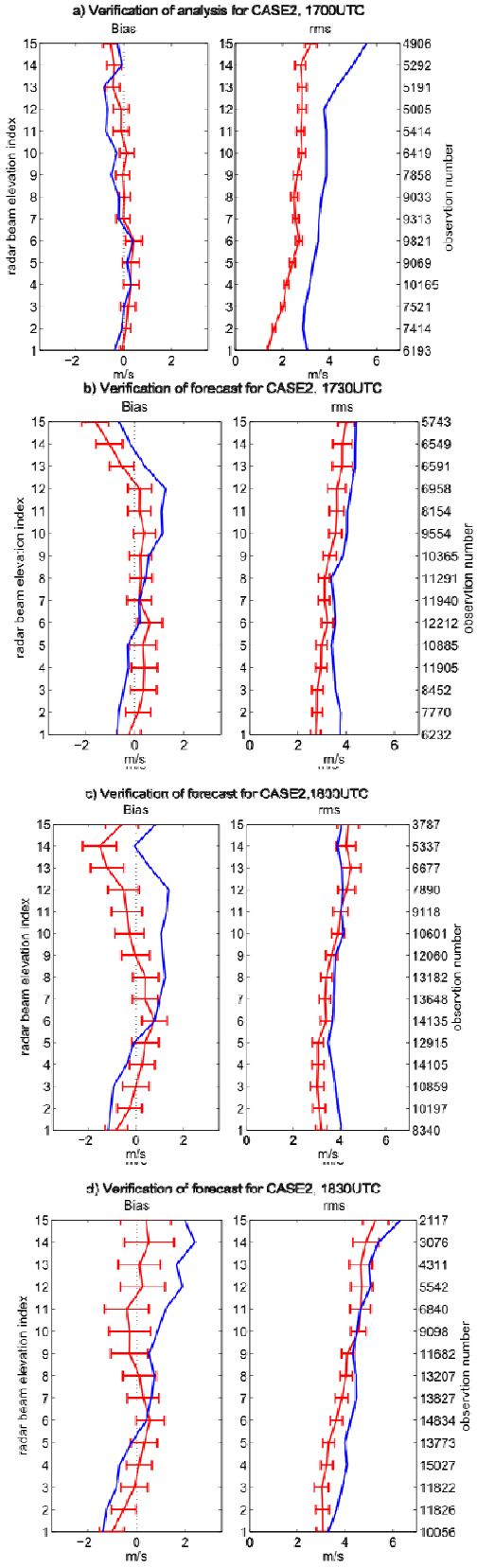

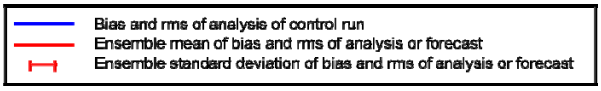

Fig. 7 Verification scores (bias and rms) of analysis and short-term ensemble forecasts against control run at different times, for the case of 12 June, 2011. Radar elevation indexes on y axis from 1 to 15 correspond to radar beam elevation angles 0.3, 0.5, 0.7, 0.9, 1.1, 1.4, 1.7, 2.0, 2.4, 2.9, 3.4, 4.1, 4.8, 5.6, 6.6 in degrees. The numbers in the right-hand-side of y axis is the amount of observations in each level.

Figure 8 are snapshots of reflectivity fields of two analysis members and the control run together with the reflectivity observations at 1700 UTC when all cycles are completed. In general, given reflectivity observations as reference, the figures of both analysis members exhibit relatively more accurate storm locations near the center and to the north of the domain, compared to the control run. It infers that the HREnKF is able to correct the storm location error to some extent. However, when the radar observes some precipitation in the southeastern area, it is missed by both analysis members and control run.

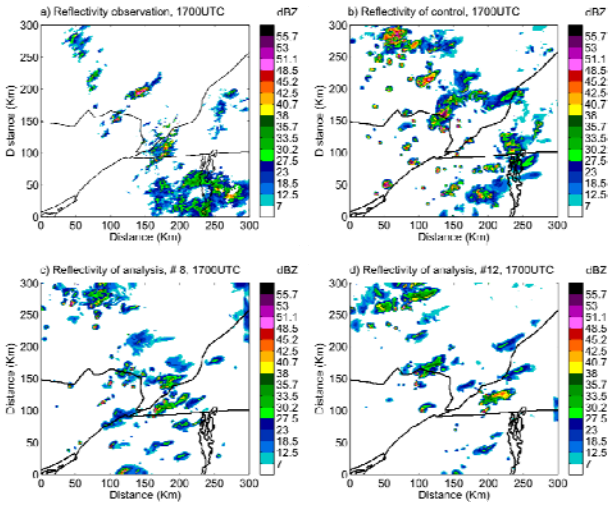

Fig. 8. Reflectivity fields of observations, control run and final analysis at 1700UTC, June 12, 2011. a) observed reflectivity at the 4th elevation angle. b) simulated reflectivity of the control run near the surface. c) simulated reflectivity of the 8th analysis member near the surface. d) simulated reflectivity of the 12th analysis member near the surface.

To have a further investigation, the convective available potential energy (CAPE) fields for the control run and the 8th member of ensemble analysis are investigated (Fig.9). CAPE describes the convective instability present in forecast fields and we stress that its computation involves unobserved variables during the data assimilation cycling. Near the center of the domain and to the east of the radar, the CAPE values in #8 analysis are much greater than in the control run, which demonstrates that the assimilation of radial velocity greatly increases the instability. In the west, the CAPE values for #8 analysis are smaller because the lack of observations over that region does not support strong instability. However, in the southeast part of the domain, both analysis and control run give small CAPE values, even though plenty of observations are available over that region. One plausible reason explaining this fact is that the cross-correlation between wind components and other variables are too weak and that the wind field is close to the truth but other fields are not. For example, as shown in Fig. 5, the unobserved humidity over the southeast area is not much affected by assimilating radial velocities. When the same problem happens to other unobserved fields, the HREnKF fails to increase the instability over that region and trigger any precipitation.

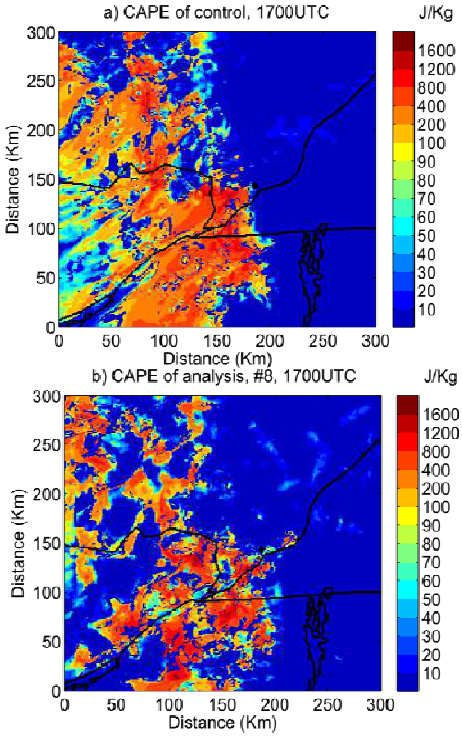

Fig.15 CAPE outputs of the control (a), and the 8th analysis member (b) of 12 June, 2011 at 1700 UTC. The black dots denote the location of the radar

5. Summary

This study introduces a High Resolution Ensemble Kalman filter (HREnKF) system designed in particular for convective-scale radar data assimilation. The observations assimilated by the HREnKF in current experiments are radial velocities from McGill Radar Observatory and covering the Montréal region. Radial velocity observations are incorporated by HREnKF every five-minutes cycle for twelve cycles during the one-hour assimilation process, by the end of which, final analyses are produced and a 1.5-h ensemble of 80 forecasts is launched.

Currently, three summer cases in 2011 are studied

to investigate the performance of the HREnKF and its impact on final analyses and short-term forecasts under different circumstances. The case which contains isolated strong small-scale storms on the 12th of June is showed in this manuscript. Even though the HREnKF only assimilates radar radial wind, our study showed that unobserved variables are also updated by the HREnKF through the error cross-correlation between observed and unobserved variables. The result showed notable increment of the humidity field in each cycle although humidity is not observed by the radar.

The indicators of ensemble spread, analysis rms and background rms exhibited sufficient ensemble spread during the cycling process when the REnKF and ensemble lateral boundary conditions are implemented. As the cycling procedure proceeds, the portion of observations kept by the background check gradually increases, given that the ensemble spread reduces, one can conclude that the model state in HREnKF gradually converges to the observations during the cycling process.

This case demonstrated that when localized convection happen, the HREnKF accounts for most of the corrections, is able to improve the location of the storms in the resulting analyses. In addition, the ensemble forecast is much better than the control run with respect to radial velocity observations, and lasts up to 90 min after forecast initiation. In addition, images of reflectivity and CAPE showed that not only the precipitation field can be changed by assimilating radial velocity, but also the entire model convective instability in a manner consistent with radar observations.

Since only radar radial wind data has been assimilated to the HREnKF system, some limitations exist in our current experiments. For instance: The update of unobserved fields relies on the cross-correlation between errors of observed and unobserved variables, which could occasionally be too weak to accomplish all necessary corrections. As a further step towards full exploitation of available radar observations, reflectivity data will be considered in addition to radial winds in the near future.

Acknowledgement

The authors would like to express their gratitude to: Prof. Frederic Fabry and Prof. Isztar Zawadzki who provided clean radar data and gave many valuable suggestions to this study.

References

Caron, J.-F., 2012: Mismatching Perturbations at the Lateral Boundaries in Limited-Area Ensemble Forecasting: A Case Study. *Mon. Wea. Rev.*, **141,** 356-374.

Chung, K.-S., I. Zawadzki, M. K. Yau, and L. Fillion, 2009: Short-Term Forecasting of a Midlatitude Convective Storm by the Assimilation of Single-Doppler Radar Observations. *Mon. Wea. Rev.*, **137,** 4115-4135.

Chung, K.-S., W. Chang, L. Fillion, and M. Tanguay, 2013: Examination of Situation-Dependent Background Error Covariances at the Convective Scale in the Context of the Ensemble Kalman Filter. *Mon. Wea. Rev.*, In Press.

Fillion, L., and S. Bélair, 2004: Tangent Linear Aspects of the Kain-Fritsch Moist Convective Parameterization Scheme. *Mon. Wea. Rev.*, **132,** 2477-2494.

Houtekamer, P. L., and H. L. Mitchell, 2001: A Sequential Ensemble Kalman Filter for Atmospheric Data Assimilation. *Mon. Wea. Rev.*, **129,** 123-137.

Houtekamer, P. L., H. L. Mitchell, G. Pellerin, M. Buehner, M. Charron, L. Spacek, and B. Hansen, 2005: Atmospheric Data Assimilation with an Ensemble Kalman Filter: Results with Real Observations. *Mon. Wea. Rev.*, **133,** 604-620.

Milbrandt, J. A., and M. K. Yau, 2005: A Multimoment Bulk Microphysics Parameterization. Part I: Analysis of the Role of the Spectral Shape Parameter. *J. Atmos. Sci.*, **62,** 3051-3064.

Saito, K., H. Seko, M. Kunii, and T. Miyoshi, 2012: Effect of Lateral Boundary Perturbations on the Breeding Method and the Local Ensemble Transform Kalman Filter for Mesoscale Ensemble Prediction. *Tellus A*, **64,** 11594.

Sun, J., and N. A. Crook, 1997: Dynamical and Microphysical Retrieval from Doppler Radar Observations Using a Cloud Model and Its Adjoint. Part I: Model Development and Simulated Data Experiments. *J. Atmos. Sci.*, **54,** 1642-1661.